

Active Galactic Nuclei and the Cosmic X-Ray Background

Eduardo Ibar

Supervisors: Dr. Rob Ivison & Dr. Philip Best

March 20, 2007

1 Active Galactic Nuclei

Active Galactic Nuclei (AGNs) are the most luminous objects in the Universe (besides Gamma-Ray Bursts). Typical spatial scales for these objects are estimated from time variability, giving sizes of around one parsec (Clavel et al. 1991, Peterson et al. 1992), similar to our solar system, but with typical luminosities 10^{11} larger than the Sun. It is believed that their energy comes from the inflow of material, through an accretion disk, into a super-massive black hole ($\sim 10^6 - 10^9 M_{\odot}$). From observations of these objects the existence of two main emission regions is inferred. A fast moving and high density region near to the black hole named the Broad Line Emission Region (BLR – Dibi 1987) characterised by a considerable broadening of the permitted spectral lines ($\text{FWHM} \approx 10^3 - 10^4 \text{ km/sec}$), and a Narrow Line Emission Region (NLR – Smith 1993), described as a relatively slow moving, low density region that could be spread over $\sim kpc$ distances from the black hole, generating narrow emission lines $< 10^2 - 10^3 \text{ km/sec}$ only.

Since an observational evidence for a relationship between the mass of the massive black holes and the velocity dispersion of galaxy bulges has been found, the study of AGNs have become fundamental part of our understanding of the formation and evolution of galaxies. In fact, it implies a tight relation between

the growing of the black hole, produced when the galaxy is active during accretion and/or black hole mergers, with the total mass of the bulge, acquired by hierarchical galaxy formation (Haehnelt & Kauffmann 2000). Hence, the determination of the history of accretion in AGNs is crucial for our understanding of how super-massive black holes and their hosts grow and evolve. So far, we lack a comprehensive model that could explain the cosmic history of galaxies from the beginning to the end.

2 Unification Model

AGNs have been studied for a long time resulting in much observational evidence for the diversity of AGN classes – Quasars, Blazars, BL Lac objects, FR I & II, Seyfert galaxies, and many others. A unified scheme for the variety of Active Galactic Nuclei (AGNs) has been proposed by Antonucci (1993) based on the differences observed in Seyfert galaxies, a class of local active galaxies which present narrow forbidden lines but could have broad permitted lines. According to this *Unification Model*, the active nucleus is surrounded by a toroidal structure composed of gas and dust, which determines dramatic spectral differences depending on our line of sight towards the central source (see Figure 1).

In the X-Ray domain, if an AGN has a neutral Hydrogen column density (N_H) in the line of

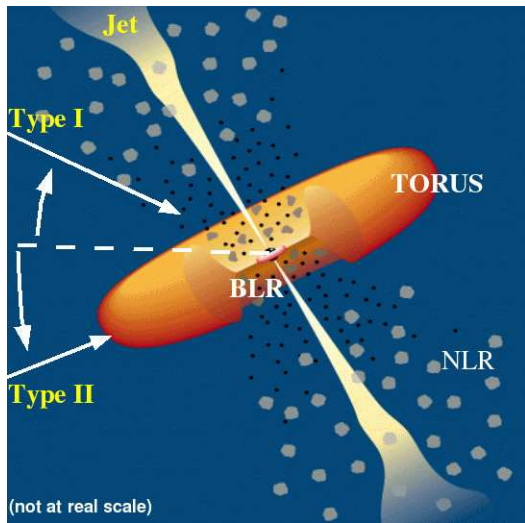


Figure 1: Scheme for the Unification Model for AGNs. The presence of the torus is the key factor for the spectral differences observed for Type I and Type II sources.

sight smaller (when viewed face-on) or larger (when viewed edge-on) than 10^{22} cm^{-2} , then the object is classified as Type I or Type II, respectively (Figure 1). On the other hand, in the optical range, the velocity dispersion of the permitted lines (such as H_α) is used to define Type I and Type II sources. By definition, a FWHM larger than 1200km/sec implies a direct view to the central BLR (Type I), but not otherwise.

The *Unification Model* is supported by a large variety of observational evidences in low redshift AGN. For example, polarised emission from Type II objects (Antonucci 1993), spatial anisotropies in the extended ionising structures (Falcke et al. 1998), photoelectric absorption and reprocessed emission in X-Rays (Lightman & Rybicki 1980), the detection of broad emission lines at IR wavelengths in Type II sources (Ruiz et al. 1994), and the reprocessed torus IR excess (Nenkova et al. 2002). At high- z , the most

clear evidence for the presence of obscured sources, as we will present, is the hard spectral nature of the CXRB.

3 Radio emission

The emission from powerful extragalactic radio ($> 1mJy$) sources is usually related to AGN activity (Condon 1984). This emission is dominated by jets coming from a central powerful AGN which generate front-shocks in the surrounding medium, producing synchrotron emission. These sources are useful for our understanding of the activity of the nuclear region and the growth of the Supermassive-Black Hole present in AGNs (therefore to galaxy evolution too; Gebhardt et al. 2001). Since massive black holes appear to reside in all massive present-day spheroids, with a mass roughly proportional to the mass of the spheroid (Kormendy & Gebhardt 2001), this suggests that black-hole and spheroid formation are intimately linked. There are strong indications that powerful radio activity, at least for steep spectrum radio sources, is only produced by the most massive black holes ($M \gtrsim 10^9 M_\odot$; Dunlop et al. 2003); the cosmic evolution of powerful radio sources may therefore offer the cleanest way to constrain the evolution of the top end of the black hole mass function.

4 UV-Optical Emission

At optical wavelengths, the torus drastically changes the spectroscopic properties depending on the line of sight towards the central engine. In the case of Type I sources, the accretion disk produces a bright contribution to the spectra, with a bump in the ultraviolet. A continuum spectral slope is seen as a result of the accretion disk emission coming from the integration of different blackbodies at different

temperatures given by the distance to the supermassive black hole. Typical broad permitted lines of 1000 – 10000km/sec evidence very large velocity dispersions from the vicinities of the nuclear region (BLR). Also, the NLR contributes to the spectrum with narrow forbidden lines (such as [OIII]) with FWHM < 1000km/sec. The galaxy host emission is negligible compared with the central emission and is basically almost impossible to observe it. On the other hand, Type II sources are characterised by an absorbed accretion disk but observed emission from the local galaxy, and narrow lines (forbidden and permitted) only, coming from the low density-slow moving material of the NLR.

5 X-Ray Emission

It is commonly believed that the X-Ray emission is produced in a 'corona' near the super-massive black hole, where low energy photons from the accretion disk are reprocessed by energetic electrons (either mildly relativistic thermal electrons or highly relativistic non-thermal electrons) via Inverse Compton Scattering. The main result of this process is an observed spectral energy distribution described by a power law, with a typical slope $\Gamma \approx 1.8$ (Turner et al. 1997, Tozzi et al. 2006), and an exponential cut-off energy at ≈ 300 keV (Matt et al. 1999). The radiation can also be reflected and/or scattered depending on the circumnuclear material distribution causing the overall spectral shape to become flatter, $\Gamma \approx 1.7$, with an apparent smaller energy cutoff (see Svensson 1996).

The dusty toroidal structure that surrounds the central source absorbs the optical, ultraviolet and soft X-Ray emission from the active nucleus. However, hard X-Ray photons (> 2 keV) can partially escape from this cold material. In fact, the hard X-Ray emission in the 2 – 10 keV band, is a well de-

termined characteristic of AGNs due to the extreme non thermal conditions that produce this radiation. This band is also used (and the best way - Mushotzky 2004) to describe the number density and evolution of AGNs in the Universe. Emission at larger wavelengths – infrared, sub-mm, radio – can also escape from the surrounding dusty media, allowing the observation of highly obscured sources which can not be detected in X-Rays. Actually, if the Hydrogen column density along the line of sight becomes larger than the inverse of the photoelectric Cross Section $\sigma_{10\text{keV}}^{-1} \approx 10^{24} \text{ cm}^{-2}$ (see Matt 2002), then the medium becomes Compton Thick ($\tau = N_H \sigma \approx 1$). In this case, the only observable emission component is coming from photons scattered and/or reflected by the circumnuclear media (Wilman & Fabian 1999).

5.1 Detailed Template for the X-Ray Emission

With the observations of X-Ray satellites like GINGA, ASCA, and BeppoSAX, different spectral components have been recognised in the X ray spectra of AGNs. The observed Spectral Energy Distribution (SED) from each point source is modelled as (see Figure 2):

$$\begin{aligned}
 F_E &= \frac{dF}{dE}(L_X, z, N_H, \Gamma) \\
 &= A \frac{L_X(1+z)}{4\pi d_L^2(z)} \left(e^{-\sigma(E_z)N_H} + \text{REF}_{\%} \right) \\
 &\quad \times \left(E_z^{-\Gamma+1} e^{-E_z/E_C} + \text{REP}(E_z) \right)
 \end{aligned} \tag{1}$$

where $E_z = E(1+z)$, A is a normalisation value so that L_X corresponds to the intrinsic integrated luminosity in the 2 – 10 keV rest-frame band (to be used together with a luminosity function), z is the redshift,

$d_L(z)$ is the luminosity distance parameterised by the assumed cosmology, $\sigma(E)$ is the effective cross section for a solar metallicity medium (Morrison & McCammon 1983) extrapolated to higher energies ($\gtrsim 10\text{keV}$) by a photoelectric bound-free cross section $\propto E^{-3}$ (note that when $\text{Log}(N_H \text{ cm}^{-2}) > 24$, Compton recoil, or Compton down scattering, becomes important at high energies). A spectral index $\Gamma = 1.9$ is used to characterise the primary emission, according to the overall results from spectral analysis of nearby active galaxies (Nandra & Pounds 1994) and with the mean value in the Lockman Hole observed by *XMM-Newton* (Mainieri et al. 2002). The high energy cut-off $E_C \approx 300\text{keV}$ is adopted from bright Seyfert galaxies and it becomes important for predicting the contribution of AGNs to the CXRB above 10keV (Ueda et al. 2003), although this value is highly unconstrained (Matt et al. 1999). $\text{REP}(E)$ is the estimated angle averaged reprocessed primary emission by Compton cold (disk) reflection, assuming a solid angle of 2π and solar abundances for all elements (dashed line from Figure 5 in Magdziarz & Zdziarski 1995). The ratio of the reflection component $\text{REP}(E)$ to the primary one is about 10% just below 7.1keV (the K edge energy of cold iron atoms) and rapidly decreases toward lower energies (0.1% at 1keV), while above 7.1keV it has a maximum of about 70% around 30keV . A $K\alpha$ line component from the ionised iron atoms is also included on the reflection component. Compton down scattering becomes important at $N_H > 10^{24}\text{cm}^{-2}$ affecting the high energy X ray photons through electron recoil, as described by Wilman & Fabian (1999). Finally, typically a reflected $\text{REF}_{\%} = 2\%$ component from the central emission is produced by warm ionised gas located above the opening angle torus.

Figure 2 shows the X-Ray template as a function of the column densities, where it is clearly seen a dramatic spectroscopic variation within the *Chandra* and *XMM-Newton* band, 0.1-10keV.

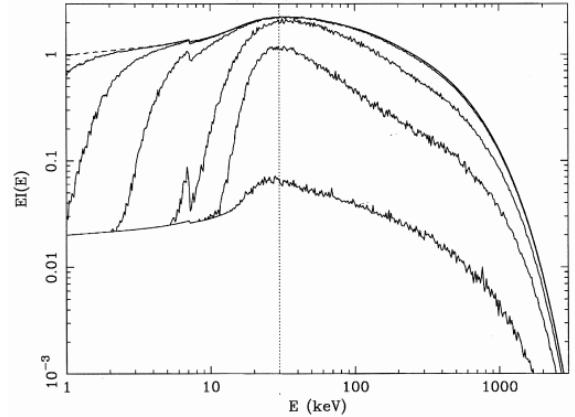


Figure 2: Template spectrum for the X-Ray emission including 2 per cent component scattered by warm ionised material. Dashed line correspond to a unobscured-Type I spectra, and the solid lines describe the effect in the spectra produced by different column densities (from left to right) $N_H = 10^{21.25}, 10^{22.25}, 10^{23.25}, 10^{24.25}, 10^{24.75}$ and $10^{25.25}\text{cm}^{-2}$. Note that all the spectra peak at $E \sim 30\text{keV}$, as the position of dotted vertical line makes clear. These spectra do not include the iron $K\alpha$ line *Figure from Wilman & Fabian (1999)*.

5.2 Hard X-Ray Luminosity Function

Using a compilation of *ASCA*, *HEAO - 1* and *Chandra* observations, Ueda et al. (2003) constructed a luminosity function for AGNs (247 sources) in the hard X ray band ($2 - 10\text{keV}$). Ueda's luminosity function shows a luminosity dependent density evolution, in which the low luminosity AGN population peaks at a lower redshift than the high luminosity sources. This is consistent with optical quasar observations in which this population peaks at redshift ~ 2 (Boyle et al. 2000).

The main impact of Ueda's work is that by using hard band detections only, it gives the best estimation of the number of AGN in the Universe (Mushotzky

2004) avoiding a possible contamination from thermal sources (such as diffuse Galactic and/or Solar system emission, intergalactic warm gas and Starburst galaxies). However, as most surveys, this luminosity function is biased against low luminosity sources, due to either, low intrinsic power or large amounts of absorption (up to 4 orders of magnitude larger in Type II than in Type I AGNs in the 2 – 10 keV rest-frame band). In fact, the demographics of the low luminosity and the highly obscured AGN populations remains unclear.

Ueda's luminosity function is defined for AGNs in the $10^{41.5} - 10^{46.5} \text{ erg sec}^{-1}$ luminosity range in the 2 – 10 keV energy range, up to $z \approx 3$, and in the $20 < \text{Log}(N_H \text{ cm}^{-2}) < 24$ range, implying that an extrapolation is needed to extract information for column densities above 10^{24} cm^{-2} (i.e. for Compton Thick sources).

X-Ray surveys are always flux limited (nowadays $F_{2-10\text{keV}}^{\text{limit}} \approx 10^{-16} \text{ erg sec}^{-1} \text{ cm}^{-2}$), and therefore biased against faint sources. This problem translates into a poorly determined faint end of the luminosity function, implying uncertainties in the contribution from highly obscured AGNs to the Cosmic X-Ray Background (CXRB). This problem is more relevant if a large population of heavily absorbed AGNs (Compton Thick sources) is needed to fit the observed CXRB spectrum.

6 AGNs and the CXRB

Having in hand a luminosity function and a spectral template for the AGN emission, we can now calculate the expected CXRB spectrum based on the integration in luminosity and redshift of the number of sources weighted by the observed redshifted spectrum.

The number of AGNs per unit redshift, per unit luminosity and per unit solid angle, is given by:

$$\frac{dN(L_X, z)}{d\text{Log}(L_X) dz d\Omega} = \frac{d\Phi(L_X, z)}{d\text{Log}(L_X)} \frac{dV_{co}(z)}{dz d\Omega} \quad (2)$$

where the first term in the right hand-side of the equation is the luminosity function and the second term is the differential co-moving cosmological volume, which weights the probability to find a source at a certain redshift given the Universe geometry.

We include a normalised function in order to distribute the number of sources in different bins of column densities (normalised up to $N_H = 10^{24} \text{ cm}^{-2}$). Therefore, the total AGN contribution to the CXRB is given by (Ueda et al. 2003):

$$\begin{aligned} F_E^{\text{CXRB}} &= \frac{dF^{\text{CXRB}}}{d\Omega dE} \\ &= \int_{z_{\min}}^{z_{\max}} \int_{\text{Log}(L_X)_{\min}}^{\text{Log}(L_X)_{\max}} \sum_{N_{Hi}=N_{H\min}}^{N_{H\max}} f(N_{Hi}) \times \\ &\quad \frac{dN(L_X, z)}{d\text{Log}(L_X) dz d\Omega} \frac{dF}{dE}(L_X, z, N_{Hi}, \Gamma) \\ &\quad d\text{Log}(L_X) dz \end{aligned} \quad (3)$$

where $\frac{dF}{dE}$ is given by the assumed AGN template (Equation 1), and $f(N_{Hi})$ is the normalised distribution of observed column densities, well defined in the $20 < \text{Log}(N_H \text{ cm}^{-2}) < 24$ range according to Ueda's luminosity function. Hence,

$$\sum_{N_{Hi}=10^{20} \text{ cm}^{-2}}^{10^{24} \text{ cm}^{-2}} f(N_{Hi}) = 1 \quad (4)$$

The results of this estimation to the CXRB are presented in Figure 3.

6.1 Results

Since in sources with $N_H > 10^{22} \text{ cm}^{-2}$ (Type II) the direct nuclear emission is highly absorbed,

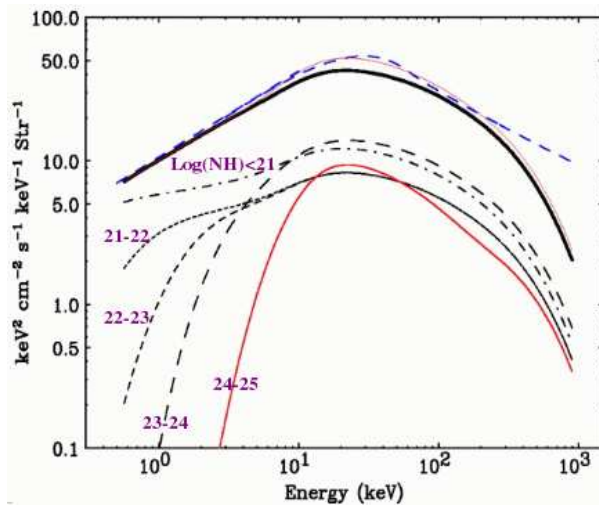


Figure 3: Composite spectrum for the contribution to the CXRB given by different obscured populations. The thick black line is the total contribution of Compton thin objects ($< 10^{24} \text{ cm}^{-2}$), and the thin red line is that including a Compton thick population assuming the same number of sources than the $\text{Log}(N_H) = 23 - 24$ range. Clearly a Compton thick population is necessary to fit the CXRB spectrum.

these sources have a hard X-Ray energy distribution (harder than typical unobscured AGN) that are essential to model the hard spectrum of the observed Cosmic X-Ray Background (CXRB) at $E < 20 \text{ keV}$ ($\Gamma_{2-10\text{keV}}^{\text{CXRB}} \approx 1.4$). This is actually the main evidence for the existence of a large number of obscured AGNs in the Universe, clearly seen in Figure 3 where the contribution of unobscured sources have a drastically different spectral slope.

From Figure 3, an extra contribution of sources with column densities larger than 10^{24} cm^{-2} is necessary to increase the CXRB flux at about $\sim 30 \text{ keV}$. This population is not possible to observe with the present telescopes, such as *Chandra* and *XMM-Newton*, because their energy range, $0.1 - 10 \text{ keV}$, ba-

sically observe the degree of reflection instead of the intrinsic emission (see Figure 2).

Previous X-Ray synthesis models for AGNs (Gilli et al. 1999,2001; Treister et al. 2004) have shown that the CXRB evidences a large fraction of highly-obscured AGNs (30% with $N_H > 10^{24} \text{ cm}^{-2}$) in all redshift – population which is still unobserved by present deep surveys due to observational limitations. On the other hand, a work by Tozzi et al. (2006) estimates a lower limit for the Compton Thick fraction of $\sim 10\%$ in the CDF-S, while Beckmann et al. (2007) find 4 Compton Thick sources of a total of 40 AGN observed with *INTEGRAL* in the 20-40 keV energy range at $z \sim 0$.

Beside of the large capabilities of deep X-Ray surveys, this Compton thick population is not easy to identify, and many other ways to tackle this population have been proposed from observations at different wavelengths.

6.2 Future Work

In order to tackle the missed Compton thick population from deep X-Ray surveys, we have been using long wavelength observations which can actually escape from the local host galaxy. In fact, radio observations can act as a useful probe of AGNs, regardless of the level of obscuration, via the identification of lobe-like morphologies or deviation of the radio spectral index ($\alpha \approx 0.75$, where $S_\nu \propto \nu^\alpha$) expected for star-forming galaxies (Ivison et al. 1999), or via anomalously high radio fluxes compared with the far-infrared/radio correlation of normal galaxies (Ibar et al. 2007).

These studies, are still in progress and a clear estimation of the number of highly obscured sources detected at radio wavelengths is not well defined yet. Although, at least we have found that 30% of the sub-mJy population is composed by radio-excess sources (those which escape from the far-infrared/radio cor-

relation). Future X-Ray counterparts, in order to identify common multi-wavelength parameters for AGNs, is the next step of analyses.

References

- [1] Antonucci, R. 1993, ARA&A, 31, 473
- [2] Boyle, B. J., Shanks, T., Croom, S. M., Smith, R. J., Miller, L., Loaring, N., & Heymans, C. 2000, MNRAS, 317, 1014
- [3] Beckmann, V., Soldi, S., Shrader, C. R., Gehrels, N. & Produit, N., 2007, ApJ, 652, 126
- [4] Clavel, J., et al. 1991, ApJ, 366, 64
- [5] Condon, J. J. 1984, ApJ, 287, 461
- [6] Dibai, E. A. 1987, Soviet Astronomy, 31, 117
- [7] Dunlop, J. S., McLure, R. J., Kukula, M. J., Baum, S. A., O’Dea, C. P., & Hughes, D. H. 2003, MNRAS, 340, 1095
- [8] Falcke, H., Wilson, A. S., & Simpson, C. 1998, ApJ, 502, 199
- [9] Gebhardt, K., et al. 2001, ApJL, 555, L75
- [10] Gilli, R., Comastri, A., Brunetti, G., & Setti, G. 1999, New Astronomy, 4, 45
- [11] Gilli, R., Salvati, M., & Hasinger, G. 2001, A&A, 366, 407
- [12] Haehnelt, M. G., & Kauffmann, G. 2000, MNRAS, 318, L35
- [13] Ibar, E., et al. *In preparation*.
- [14] Ivison, R., Smail, I., Blain, A., Kneib, J.-P., & Frayer, D. 1999, ApSS, 266, 285
- [15] Kormendy, J., & Gebhardt, K. 2001, AIP Conf. Proc. 586: 20th Texas Symposium on relativistic astrophysics, 586, 363
- [16] Lightman, A. P., & Rybicki, G. B. 1980, ApJ, 236, 928
- [17] Magdziarz, P., & Zdziarski, A. A. 1995, MNRAS, 273, 837
- [18] Mainieri, V., Bergeron, J., Hasinger, G., Lehmann, I., Rosati, P., Schmidt, M., Szokoly, G., & Della Ceca, R. 2002, A&A, 393, 425
- [19] Matt, G., et al. 1999, A&A, 341, L39
- [20] Matt, G. 2002, Royal Society of London Philosophical Transactions Series A, 360, 2045
- [21] Morrison, R., & McCammon, D. 1983, ApJ, 270, 119
- [22] Mushotzky, R., 2004, astro-ph/0405144
- [23] Nandra, K., & Pounds, K. A. 1994, MNRAS, 268, 405
- [24] Nenkova, M., Ivezić, Ž., & Elitzur, M. 2002, ApJ, 570, L9
- [25] Peterson, B. M., et al. 1992, ApJ, 392, 470
- [26] Ruiz, M., Rieke, G. H., & Schmidt, G. D. 1994, ApJ, 423, 608
- [27] Smith, S. J. 1993, ApJ, 411, 570
- [28] Svensson, R. 1996, A&A, 120, 475
- [29] Tozzi, P., et al. 2006, A&A, 451, 457
- [30] Treister, E., et al. 2004, ApJ, 616, 123
- [31] Turner, T. J., George, I. M., Nandra, K., & Mushotzky, R. F. 1997, ApJS, 113, 23

[32] Ueda, Y., Akiyama, M., Ohta, K., & Miyaji, T.
2003, *ApJ*, 598, 886

[33] Wilman, R. J., & Fabian, A. C. 1999, *MNRAS*,
309, 862